Backbone and methyl resonances assignment of the 87 kDa prefoldin from Pyrococcus horikoshii

Ricarda Törner, Faustine Henot, Rida Awad, Pavel Macek, Pierre Gans, Jérôme Boisbouvier

Backbone and methyl resonances assignment of the 87 kDa prefoldin from Pyrococcus horikoshii

Ricarda Törner*, Faustine Henot, Rida Awad, Pavel Macek, Pierre Gans, Jerome Boisbouvier*

Univ. Grenoble Alpes, CNRS, CEA, Institut de Biologie Structurale (IBS),
71, Avenue des Martyrs, F-38044 Grenoble, France.

* correspondence to be addressed to: ricarda.toerner@ibs.fr or jerome.boisbouvier@ibs.fr

Abstract

Prefoldin is a heterohexameric protein assembly which acts as a co-chaperonin for the well conserved Hsp60 chaperonin, present in archaebacteria and the eukaryotic cell cytosol. Prefoldin is a holdase, capturing client proteins and subsequently transferring them to the Hsp60 chamber for refolding. The chaperonin family is implicated in the early stages of protein folding and plays an important role in proteostasis in the cytosol. Here, we report the assignment of $^{1}H_{N}$, ^{15}N, $^{13}C'$, $^{13}C_{\alpha}$, $^{13}C_{\beta}$, $^{1}H_{methyl}$, and $^{13}C_{methyl}$ chemical shifts of the 87 kDa prefoldin from the hyperthermophilic archaeon *Pyrococcus horikoshii*, consisting of two α and four β subunits. 100% of the [^{13}C, ^{1}H]-resonances of A^{β}, $I^{\delta1}$, $L^{\delta2}$, $T^{\gamma2}$, $V^{\gamma2}$ methyl groups were successfully assigned for both subunits. For the β-subunit, showing partial peak doubling, 80% of the backbone resonances were assigned. In the α subunit, large stretches of backbone resonances were not detectable due to slow (μs-ms) time scale dynamics. This conformational exchange limited the backbone sequential assignment of the α subunit to 57% of residues, which corresponds to 84% of visible NMR signals.

Key words: *Pyrococcus horikoshii*, prefoldin, co-chaperonin, methyl, backbone, NMR, assignment

Biological context

Prefoldin (PFD) has first been described in 1998, as a key factor in the maturation of actin and tubulin in yeast, due to its interaction with type II chaperonins (Vainberg et al. 1998). It acts as a co-chaperonin by delivering unfolded protein substrates to the ATP-fuelled chaperonin complex, where refolding takes place. Chaperonins are involved in proteostasis by acting at early stages of folding (Saibil 2013). Also known as Hsp60 (Heat shock protein, 60 kDa), due to the size of their constituent subunits, chaperonins are composed of two rings, formed by 7-9 subunits each, placed back-to-back. Each ring encloses a cavity in which protein folding takes place. Group II chaperonins, having an additional helical protrusion to close their folding chamber, do not need a co-chaperonin for their closure mechanism, in contrast to group I chaperonins (co-chaperonin Hsp10). Nevertheless, group II chaperonins are assisted in the protein folding mechanism by the co-chaperonin PFD, which functions as a holdase and transfers unfolded protein into the chaperonin cavity (Yébenes et al. 2011). Consistent with the presence of type II chaperonins in archaea, PFD homologues in archaea were identified by sequence alignment (Leroux 1999). Whilst the chaperonin type II-prefoldin system is present in the cytosol of eukarya and archaea, type I chaperonins and their co-chaperonin are present in eukaryotic organelles and eubacteria, which shows the fundamental and universal nature of this chaperone system.

Although involvement in cell skeleton maturation is seen as prefoldins major role in the eukaryotic cytoplasm (Lundin et al. 2008; Lee et al. 2011), it is also involved in the assembly of other cytoplasmic complexes and promotes proteolysis and degradation (Comyn et al. 2016). PFD was also shown to play a role in prevention of the aggregation process of amyloidogenic proteins involved in Alzheimer, Parkinson and Huntington's disease, (Sakono et al. 2008; Sörgjerd et al. 2013; Tashiro et al. 2013; Takano et al. 2014) and besides these functions in the cytoplasm, prefoldin and complexes containing prefoldin subunits are found in the nucleus where they play a role in gene transcription (See for review Millán-Zambrano and Chávez 2014). In archaea, with a more limited chaperone system and no actin or tubulin present, the chaperonin-prefoldin system plays an even more versatile role as it has been shown that archaic PFD stabilizes a large array of substrate proteins (Leroux 1999). Beyond its biological role it has been recognized in biotechnology that prefoldins can be used for the synthesis and transport of nanomaterials (Shokuhfar et al. 2012; Djohan et al. 2019).

In archaea, the prefoldin complex is formed by two α subunits and four β subunits. The structure of PFD from *Methanobacterium thermoautotrophicum* was resolved by X-ray crystallography, revealing the characteristic "jellyfish-like" architecture of PFD (Siegert et al. 2000). The core is comprised of two β barrels to which β and α subunits contribute one or two β hairpins, respectively. Six coiled coils, formed by two α helices each, protrude, which terminate on both N- and C- terminus in 3 to 10 residues long random coils. The four β subunits have the same sequence, but are not structurally equivalent, as they can either be preceded or followed by an α subunit in the assembly, and therefore give rise to two different sets of NMR signals (denoted β and β').

The interaction between prefoldin and its client substrates is described as a clamp-like action of the coiled coil α helices, engaging especially the β-subunits, mediated by hydrophobic residues at the distal ends of the "tentacles" (Lundin et al. 2004; Ohtaki et al. 2008). Negative stain electron microscopy located bound actin inside the cavity of human prefoldin, attached to the tips of the α helices (Martín-Benito et al. 2002). For archaic prefoldin different binding modes were suggested, depending on client protein size, resulting in the engagement of more subunits with increasing substrate size. Whereas proteins at the size of insulin (5.7 kDa) are encapsulated in the prefoldin cavity (Ohtaki et al. 2008), proteins of 14 kDa and upwards are found to protrude from the coiled coils of prefoldin (Martín-Benito et al. 2007). Interaction with the chaperonin was found to be mediated via the same interaction interface as substrate binding (Martín-Benito et al. 2002; Zako et al. 2006, 2016). The transfer of substrate protein between PFD and chaperonin was described as a handoff process, as the release of substrate proteins from PFD is facilitated in the presence of chaperonin (Zako et al. 2005).

Here we present the resonance assignment of the $^{1}H_{N}$, ^{15}N, $^{13}C'$, $^{13}C_{\alpha}$, $^{13}C_{\beta}$, $^{1}H_{methyl}$, and $^{13}C_{methyl}$ chemical shifts of prefoldin from *Pyrococcus Horikoshii*. This assignment is a prerequisite for investigation of the chaperone mechanism by NMR, and will enable a more detailed study of prefoldins interaction with Hsp60 and client proteins.

Methods and experiments

Protein expression and purification

E. coli BL21 (DE3) cells transformed with pET23c plasmids encoding either for the α or β subunit of PFD from *Pyrococcus horikoshii*, were used for protein expression. Cells were progressively adapted to M9/$^{2}H_2O$ media in three stages over 24 h (M9 in H_2O, M9 in 50% H_20 + 50% $^{2}H_2O$, M9 in $^{2}H_2O$). In the final culture the bacteria were grown at 37°C in M9 media prepared with 99.85% $^{2}H_2O$ (Eurisotop), 2 g/L of deuterated D-glucose and 1 g/L NH_4Cl. U-[^{2}H, ^{13}C, ^{15}N] /U-[^{2}H, ^{12}C, ^{14}N]-labelled subunits were produced by combining U-[^{2}H,^{13}C]-glucose (CIL)/ U-[^{2}H]-glucose (Isotec) and $^{15}NH_4Cl$ (CIL)/$^{14}NH_4Cl$ (Sigma-Aldrich) as carbon and nitrogen source accordingly. For uniformly labelled samples, protein production was induced by 1 mM of IPTG at OD_{600nm}=0.8 and the expression was performed at 37°C for 3 h. In order to produce specifically methyl-labelled samples, adapted cells grown in M9/$^{2}H_2O$ medium were supplied with labelled precursors at precise time-intervals before induction:

For production of U-[^{2}H, ^{12}C, ^{15}N], A-[$^{13}CH_3$]$^{\beta}$, I-[$^{13}CH_3$]$^{\delta1}$, L-[$^{13}CH_3$]$^{\delta2}$, V-[$^{13}CH_3$]$^{\gamma2}$, T-[$^{13}CH_3$]$^{\gamma2}$ labelled subunits U-[^{2}H]-glucose (Sigma Aldrich) was used as carbon source and 1 g/L $^{15}NH_4Cl$ (CIL) as nitrogen source. When the O.D. at 600 nm reached 0.7, a solution containing 2-[^{13}C]methyl-4-[$^{2}H_3$]-acetolactate (NMR-Bio) was added for the stereospecific labelling of pro-*S* $L^{\delta2}$ and $V^{\gamma2}$ methyl groups (240 mg/L) (Gans et al. 2010). 40 min later 3-[^{13}C]-2-[^{2}H]-L-Alanine, (*S*)-2-hydroxy-2-(2'-[^{13}C],1'-[$^{2}H_2$])ethyl-3-oxo-4-[$^{2}H_3$]-butanoic acid (NMR-Bio) and 2,3-(^{2}H) 4-(^{13}C)-L-Threonine (NMR-Bio) were added to a final concentration of 250 mg/L, 100 mg/L and 50 mg/L respectively (Kerfah et al. 2015a; Ayala et al. 2020) for the simultaneous labelling of $I^{\delta1}$, A^{β}, $T^{\gamma2}$ methyl groups. 20 min afterwards protein production was induced by IPTG (1 mM) and protein expression was performed at 37°C for 3 h.

For production of U-[^{2}H, ^{15}N, ^{13}C], A-[1, 2-$^{13}C_2$, $^{13}C^{1}H_3$-β], V-[1, 2, 3-$^{13}C_3$, $^{13}C^{1}H_3$-pro-*S*], L-[1, 2, 3, 4-$^{13}C_4$, $^{13}C^{1}H_3$-pro-*S*], I-[1, 2, 3, 4-$^{13}C_4$, $^{13}C^{1}H_3$- δ_1] β subunit, U-[^{2}H,^{13}C]-glucose and $^{15}NH_4Cl$ (CIL) were used. Stereospecific labelling of pro-*S* $Leu^{\delta2}$ and $Val^{\gamma2}$ methyl groups was achieved with 172 mg/L 1, 2, 3-[$^{13}C_3$]-2-[$^{13}CH_3$]-2-[$O^{2}H$]-3-oxo-4, 4, 4-[$^{2}H_3$]-butanoate (Henot et al. submitted) followed 40 minutes later by the addition of 250 mg/L U-[^{13}C]-2-(^{2}H)-L-Alanine (NMR-Bio) and 60 mg/L of (*S*)-2-hydroxy-2-(1',1'-[$^{2}H_2$], 1', 2'-[$^{13}C_2$])ethyl-3-oxo-1,2,3-[$^{13}C_3$]-4,4,4-[$^{2}H_3$]butanoate (Kerfah et al. 2015b) used for labelling of A-[$^{13}CH_3$]$^{\beta}$, I-[$^{13}CH_3$]$^{\delta1}$ methyl

groups (Kerfah et al. 2015a). 20 min afterwards protein production was induced by IPTG (1 mM) and protein expression was performed at 37°C for 3 h.

The purification protocol of prefoldin subunits was adapted from (Okochi et al. 2002) and is described in an earlier publication (Törner et al. 2020). Subunits were expressed and purified separately, then combined and re-purified, allowing for combination of labelled/unlabelled subunits in one sample. Final NMR-buffer condition for PFD samples was 50 mM Tris at pH 8.5 and 100 mM NaCl in 100% $^{2}H_2O$ or 90% H_2O/10% $^{2}H_2O$.

NMR spectroscopy

U-[^{2}H, ^{13}C, ^{15}N] PFD samples, labelled on α or β subunit, were loaded in 4 mm shigemi tube at a concentration of *c.a.* 200 μM. Full sets of BEST-TROSY 3D triple resonance experiments were acquired at 70°C on a Bruker Avance III HD spectrometer equipped with a cryogenic probe and operating at a ^{1}H frequency of 850 MHz (HNCA, HN(CA)CB, HNCO, HN(CA)CO), 700 MHz (HN(CO)CA) or 600 MHz (HN(COCA)CB) for ~ 3 days each (Lescop et al. 2007; Favier and Brutscher 2019). Data were processed and assigned using nmrPipe/nmrDraw (Delaglio et al. 1995) and CcpNmr (Vranken et al. 2005).

Methyl-labelled samples were lyophilized, re-suspended in ultra-pure $^{2}H_2O$ and loaded in 4 mm shigemi tubes at a concentration of *c.a.* 200 μM. A 3D HCC HMQC-NOESY-HMQC experiment (Tugarinov et al. 2005) was acquired at 70°C on a Bruker Avance III HD spectrometer equipped with a cryogenic probe and operating at a ^{1}H frequency of 950 MHz and methyl group assignment was performed by comparison with the crystal structure of PFD from *Pyrococcus horikoshii* (Ohtaki et al. 2008) with the automated methyl assignment software MAGIC (Monneau et al. 2017). These results were cross-validated or completed using a special labelling-scheme to distinguish inter- and intra-chain NOEs (Törner et al. 2020). Furthermore 3D '*out and back*' HCC, HC(C)C and HC(CC)C- experiments (Tugarinov et al. 2003; Ayala et al. 2009; Mas et al. 2013) were acquired (at 70°C and a ^{1}H frequency of 950 MHz) in order to connect (^{13}C,^{1}H)-methyl signals to backbone ^{13}Cα and ^{13}Cβ resonances using PFD-samples (~200 μM) labelled with linear ^{13}C-chains connecting backbone atoms to $^{13}CH_3$-labelled methyl groups. Table 1 is summarizing for each sample the different NMR experiments acquired.

Assignment and data deposition

The NMR assignment of PFD complex from *Pyrococcus horikoshii* presents some spectroscopic challenges which were overcome by combining multiple state-of-the-art assignment techniques. For the α subunit, only 104 signals out of the 148 expected ones were detected in the 2D ^{15}N-TROSY (Fig 1 a), while most of the methyl group resonances were visible in the 2D methyl TROSY (57 correlations observed for 58 A^{β}, $I^{\delta1}$, $L^{\delta2}$, $V^{\gamma2}$, $T^{\gamma2}$ $^{13}C^{1}H_3$-labelled methyl groups). Therefore, we decided to first assign methyl groups based on observed NOEs and the PFD X-ray structure (Fig. 1b, 1c and 1d) (PDB structure 2ZDI). To identify the amino acid type corresponding to each methyl signal, we produced in small scale three different samples with complementary $^{13}CH_3$-labelling schemes (MTI, IAV, LV) and compared the corresponding 2D methyl-TROSY spectra. 220 NOE cross-peaks corresponding to 139 methyl pairs were detected in a 3D HMQC-NOESY-HMQC acquired on perdeuterated sample of PFD specifically $^{13}CH_3$-labelled on A^{β}, $I^{\delta1}$, $L^{\delta2}$, $V^{\gamma2}$ and $T^{\gamma2}$ methyl groups of the α subunits. The inter-methyl NOE connectivities, the residue-types assignment of each methyl signal and the known 3D structure (PDB: 2ZDI) were used as input data to assign 100% of visible methyl groups using the software MAGIC (Monneau et al. 2017). Only Ala-132 remains unassigned, but no extra resonances were detected in 2D methyl TROSY, indicating that the signal for this last methyl group is either not detectable or overlapped with the signal of Ala-129 (a methyl distant by less than 6 Å from Ala-132 methyl, for which the only NOE detected is with L11).

With 30% of the expected signal missing in the 2D ^{15}N-TROSY, the assignment of α subunit backbone resonances was more challenging. Therefore we decided to complement a set of six triple resonance experiments (3D-BEST-TROSY HNCA, HN(CA)CB, HNCO, HN(CA)CO, HN(CO)CA and HN(COCA)CB (Lescop et al. 2007; Favier and Brutscher 2019), acquired on U-[^{2}H, ^{13}C, ^{15}N] sample with 3D 'out-and back' HCC, HC(C)C and HC(CC)C experiments acquired on a U-[^{2}H, ^{15}N, ^{13}C] labelled sample, including specifically labelled A-[1, 2-$^{13}C_2$, $^{13}C^{1}H_3$-β] and I-[1, 2, 3, 4-$^{13}C_4$, $^{13}C^{1}H_3$-δ_1] residues. These last experiments enabled to connect unambiguously previously assigned A^{β}, $I^{\delta1}$ methyl groups to corresponding Cβ and Cα resonances, offering multiple starting points for sequential assignment. The set of triple resonance experiments were used to extend and cross-validate the assignment, leading to the sequence specific assignment of 84% of the detectable backbone resonances (i.e. 59% of α subunit residues). The 44 amino acids, whose backbone resonances were not assigned, are located in the N- and C-terminus as well as in

hinge regions between β-hairpins and α-helices (Fig. 1b), suggesting that dynamics in the µs-ms regime may have broadened backbone resonances beyond detection in these particularly flexible regions. As all the methyl groups were assigned in this subunit, we used a MQ-CH_3-CPMG experiment (Korzhnev et al. 2004) to confirm that these unassigned backbone segments were displaying conformational exchange in the intermediate regime (Fig. 1e and 1f).

Contrary to the α subunit, the β subunit shows partial resonances doubling (131 and 70 signals were detected in 2D ^{15}N- and $^{13}CH_3$-TROSY, while the number of expected signals are 117 and 49, respectively) because of the non-equivalence of the beta subunits in the structure. The differences between the β subunits (noted β and β' subunits), are mainly in the core β-barrels of PFD, resulting in different chemical environments. (Fig. 2a and 2b). Sequential assignment of the β-subunit backbone was performed using triple resonance experiments (3D-BEST-TROSY HNCA, HN(CA)CB, HNCO, HN(CA)CO, HN(CO)CA and HN(COCA)CB (Lescop et al. 2007; Favier and Brutscher 2019), enabling assignment of 80% of non-proline residues. 13 residues were found with two resonances due to the asymmetry of the PFD complex. (Fig. 3)

Automatic structure-based assignment of methyl resonances in the β subunit from NOEs was not feasible due to partial peak doubling, which cannot be taken into account in the available softwares. Therefore, we acquired 'out and back' HCC, HC(C)C and HC(CC)C experiments to transfer assignment from backbone to A^{β}, $I^{\delta1}$, $L^{\delta2}$, $V^{\gamma2}$ methyl groups using U-[^{2}H, ^{15}N, ^{13}C], A-[1, 2-$^{13}C_2$, $^{13}C^1H_3$- β], V-[1, 2, 3-$^{13}C_3$, $^{13}C^1H_3$-pro-*S*], L-[1, 2, 3, 4-$^{13}C_4$, $^{13}C^1H_3$-pro-*S*], I-[1, 2, 3, 4-$^{13}C_4$, $^{13}C^1H_3$- δ_1] labelled sample. These first assigned methyl groups were used as starting points for manual assignment of intermethyl NOE network detected using a perdeuterated sample of PFD specifically $^{13}CH_3$-labelled on A^{β}, $I^{\delta1}$, $L^{\delta2}$, $V^{\gamma2}$ and $T^{\gamma2}$ methyl groups of β subunits (Fig. 2c). 85% of methyl groups could be assigned using 3D NOESY and HCC-types experiments, but 8 leucine residues, located in the leucine zipper part of the α helices could not be assigned due to their similarities in both Cα/Cβ chemical shifts and methyl connectivity networks. Hence, the mutants L15M, L36M, L43M, L86M and L75M were generated, which helped to unambiguate the assignment possibilities and therefore allowed for completion of the methyl assignments of the remaining 8 methyl groups.

As peak doubling of the β subunits arises from different interactions between the subunits, the unique NOE connectivity networks were used to distinguish the subunit preceded by an α subunit (noted β) from the one followed by an α subunit in the β barrel arrangement (noted β'- Fig.

2a). Optimized ^{13}C-edited NOESY experiments combined with a specific labelling scheme on α and β subunit allowed to distinguish inter- from intra-chain NOEs in the crowded spectrum, thereby facilitating this step (Törner et al. 2020). This distinction in β/β' assignment was transferred to the backbone via the connection of Cα /Cβ with methyl resonances (Fig. 3). Residues I107, T104, L103, I26, L22, L15 and L12 located in the distal α-helical region of the β subunit also show peak doubling, which was not assigned specifically to β/β' as this doubling most probably arises due to slow dynamics of the distal helical regions.

The assignment of chemical shifts of PFD subunits α and β has been deposited into BMRB (https ://www.bmrb.wisc.edu/) with accession number 50845.

Funding

This work used the high field NMR facility at the Grenoble Instruct-ERIC Center (ISBG; UMS 3518 CNRS-CEA-UGA-EMBL) within the Grenoble Partnership for Structural Biology (PSB). Platform access was supported by FRISBI (ANR-10-INBS-05-02) and GRAL, a project of the University Grenoble Alpes graduate school (Ecoles Universitaires de Recherche) CBH-EUR-GS (ANR-17-EURE-0003). IBS acknowledges integration into the Interdisciplinary Research Institute of Grenoble (IRIG, CEA). This work was supported by the French National Research Agency in the framework of the "*Investissements d'avenir*" program (ANR-15-IDEX-02).

Ethics declarations

Conflict of interest

The authors declare no conflict of interest.

Table 1: Summary of NMR experiments acquired for each Prefoldin sample

U-[^{2}H,^{15}N,^{13}C]-Prefoldin α-labelled/β-unlabelled or α-unlabelled/β-labelled		
2D-BEST-TROSY[a]	1 h	850 MHz
3D-BEST-HNCO[a]	1 day	850 MHz
3D-BEST-HNCA[a]	3 days	850 MHz
3D-BEST-HN(CA)CB[a]	3.5 days	850 MHz
3D-BEST-HNCACO[a]	3 days	850 MHz
3D-BEST-HN(CO)CA[a]	3 days	700 MHz
3D-BEST-HN(COCA)CB[a]	4 days	600 MHz
U-[^{2}H,^{15}N], [$^{13}CH_3$]-A$^{\beta}$I$^{\delta1}$LV^{proS}T$^{\gamma2}$ α-labelled/β-unlabelled or α-unlabelled/β-labelled		
3D HCC HMQC-NOESY-HMQC[b]	3 days	950 MHz
2D-SOFAST-methyl-TROSY[c]	0.5 h	950 MHz
U-[^{2}H,^{15}N,^{13}C], [$^{13}CH_3$]-A$^{\beta}$I$^{\delta1}$LV^{proS}, [$^{12}C^{2}H_3$]- LV^{proR} α-unlabelled/β-labelled		
3D HCC[d]	1 day	950 MHz
3D HC(C)C[d]	1.5 days	950 MHz
3D HC(CC)C[d]	2 days	950 MHz
U-[^{2}H,^{15}N,^{13}C], [$^{13}CH_3$]-A$^{\beta}$I$^{\delta1}$LV^{proR}, [$^{12}C^{2}H_3$]- LV^{proS} α-labelled/β-unlabelled		
3D HCC[d]	1 day	950 MHz
3D HC(C)C[d]	1.5 days	950 MHz
3D HC(CC)C[d]	2 days	950 MHz
U-[^{2}H,^{15}N], [$^{13}CH_3$]-I$^{\delta1}$M$^{\varepsilon}$T$^{\gamma2}$ or A$^{\beta}$I$^{\delta1}$V^{proS} or LV^{proS} for α- or β-labelled		
2D-SOFAST-methyl-TROSY[c]	0.5 h	950 MHz
U-[^{2}H,^{15}N], [$^{13}CH_3$]-LV^{proS} β-subunit mutants L15M, L36M, L43M, L86M, L75M		
2D-SOFAST-methyl-TROSY[c]	0.5 h to 12 h	950 MHz

a. (Lescop et al. 2007; Favier and Brutscher 2019); b. (Tugarinov et al. 2005); c. (Tugarinov et al. 2003; Amero et al. 2009); d. (Tugarinov et al. 2003; Ayala et al. 2009; Mas et al. 2013).

Figure Legends

Figure 1: Assignment of PFD α-subunit. a ^{15}N-TROSY spectrum of the α subunits in the 87 kDa PFD complex acquired at a ^{1}H frequency of 850 MHz and 70°C. Only 104 signals from 148 backbone residues are visible. Assigned signals are annotated with corresponding residue numbers. **b** Structure of the PFD heterohexamer (PDB:2ZDI) with α subunits in blue, β subunits in green. Unassigned NH-correlations on the α subunit are shown in black, methyl groups are shown as red spheres. On panel **c** a zoom around Ile-73-δ1 methyl group (red sphere) is presented. Neighboring methyl groups connected to the Ile-73-δ1 methyl group by ^{1}H-^{1}H NOEs are represented by blue spheres. Panel **d** displays the 2D-strip extracted at the ^{1}H frequency of Ile-73-δ1 methyl group from 3D HMQC-NOESY-HMQC acquired at 70°C on a spectrometer operating at a ^{1}H frequency of 950 MHz using a perdeuterated sample of PFD specifically $^{13}CH_3$-labelled on A^{β}, $I^{\delta1}$, $L^{\delta2}$, $V^{\gamma2}$ and $T^{\gamma2}$ methyl groups. **e** and **f** panels display CPMG-relaxation dispersion curves for V17 and V128 γ_2-methyl groups. MQ-CH_3-CPMG experiments (Korzhnev et al 2004) were recorded on the methyl-labelled samples with a relaxation delay of 30 ms and a maximum CPMG frequency of 2000 Hz, on a NMR spectrometer operating at a ^{1}H frequency of 700 MHz. Data was processed using nmrPipe/nmrDraw and analysed with chemEx (https://github.com/gbouvignies/ChemEx).

Figure 2 Assignment of PFD β-subunit. a Structure of the PFD heterohexamer (PDB:2ZDI) with α subunits in blue, β subunits in green. Two types of β subunit are distinguished, the subunit preceded by an α subunit (noted β) and the one followed by an α subunit (noted β'). Examples of different methyl-methyl proximities between the subunits due to the arrangement of the heterohexameric $\alpha_2\beta_4$ PFD complex are shown for L62 and L62'. In **b** corresponding 2D-strips extracted from a 3D HMQC-NOESY-HMQC at the ^{1}H frequency of L62 and L62' δ2 methyl groups are depicted. Experiment was acquired using a perdeuterated sample of PFD specifically $^{13}CH_3$-labelled on A^{β}, $I^{\delta1}$, $L^{\delta2}$, $V^{\gamma2}$ and $T^{\gamma2}$ methyl groups at 70°C on a spectrometer operating at a ^{1}H frequency of 950 MHz. Pannel **c** presents 2D extracts from 3D 'out-and back' HCC, HC(C)C and HC(CC)C, HNCA, HN(CO)CA and HN(CA)CB experiments. In blue C_{α} (i-1) resonances, red C_{α} (i) resonances and green C_{β} (i) resonances. Optimally labelled PFD samples were used to transfer assignment from backbone to methyl groups of L62, I63 and V64 of β and β' subunits. **d** $^{13}CH_3$-TROSY spectrum of β subunit in the 87 kDa PFD complex acquired at a ^{1}H frequency of 950

MHz and 70°C. 70 methyl signals (annotated with corresponding residue numbers) were detected for the β /β'-subunits in the PFD complex specifically $^{13}CH_3$-labelled on the 49 A^{β}, $I^{\delta 1}$, $L^{\delta 2}$, $V^{\gamma 2}$ and $T^{\gamma 2}$ methyl groups. The inlet in **d** displays examples of mutant spectra (L15M and L43M) in dark purple, used to complete the NOE/HCC-based assignment of methyl groups for the β /β'-subunits. For comparison the wild type spectra are displayed in magenta.

Figure 3 Assignment of NH resonances of PFD β-subunit. ^{15}N-TROSY spectrum of β subunit in the 87 kDa PFD complex acquired at a ^{1}H frequency of 850 MHz and 70°C. 131 signals were detected the β /β'-subunits in the PFD complex. Assigned signals are annotated with corresponding residue numbers and residues which could be assigned unambiguously to β /β' are annotated in red.

Figure1

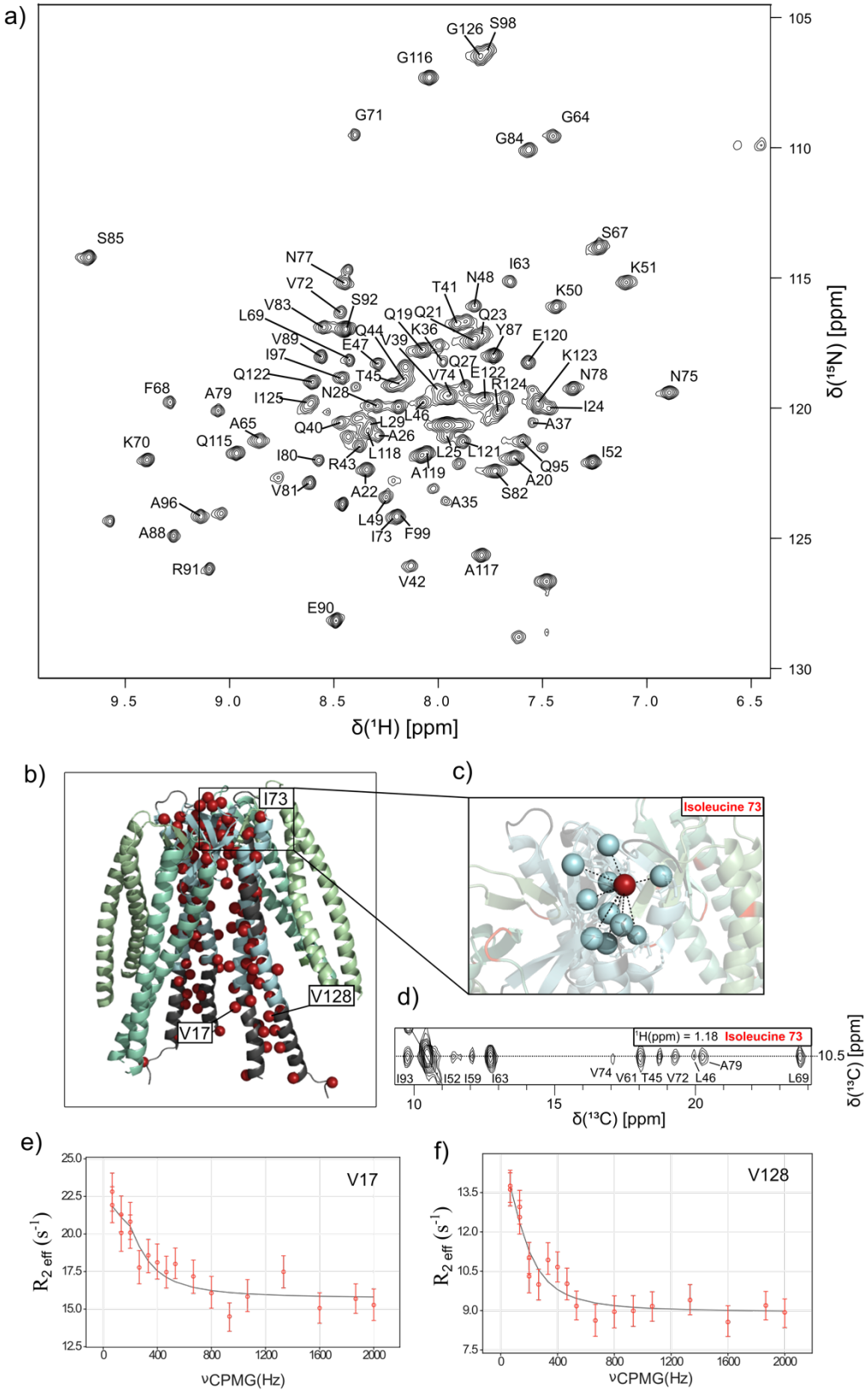
a)
δ(¹H) [ppm]
δ(¹⁵N) [ppm]
b)
I73
V128
V17
c)
Isoleucine 73
d)
¹H(ppm) = 1.18 Isoleucine 73
δ(¹³C) [ppm]
δ(¹³C) [ppm]
e)
V17
R2 eff (s⁻¹)
νCPMG(Hz)
f)
V128
R2 eff (s⁻¹)
νCPMG(Hz)

Figure2

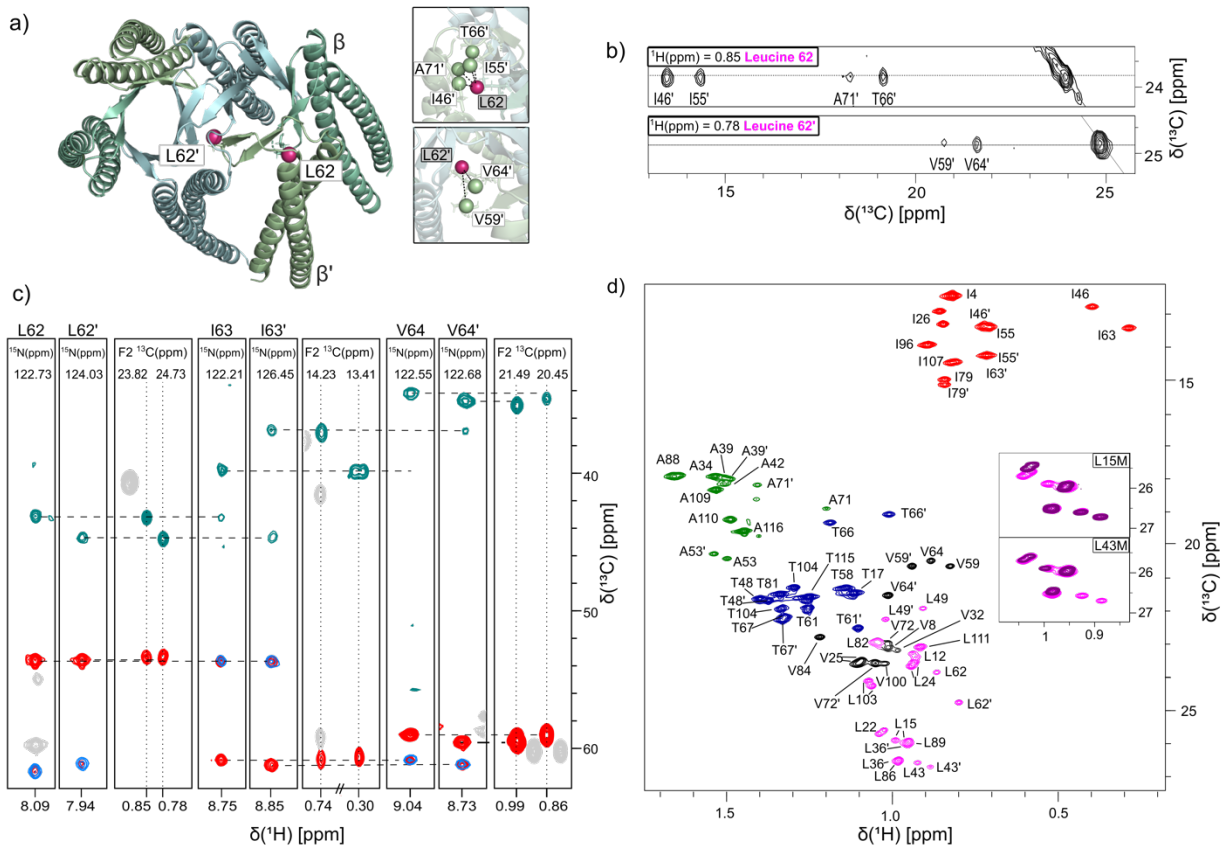
a)
β
β'
L62'
L62
T66'
A71'
I55'
I46'
L62
L62'
V64'
V59'
b)
¹H(ppm) = 0.85 Leucine 62
¹H(ppm) = 0.78 Leucine 62'
I46'
I55'
A71'
T66'
V59'
V64'
δ(¹³C) [ppm]
δ(¹³C) [ppm]
c)
L62
L62'
I63
I63'
V64
V64'
¹⁵N(ppm)
F2 ¹³C(ppm)
122.73
124.03
23.82 24.73
122.21
126.45
14.23 13.41
122.55
122.68
21.49 20.45
δ(¹³C) [ppm]
δ(¹H) [ppm]
d)
δ(¹³C) [ppm]
δ(¹H) [ppm]
L15M
L43M

Figure 3

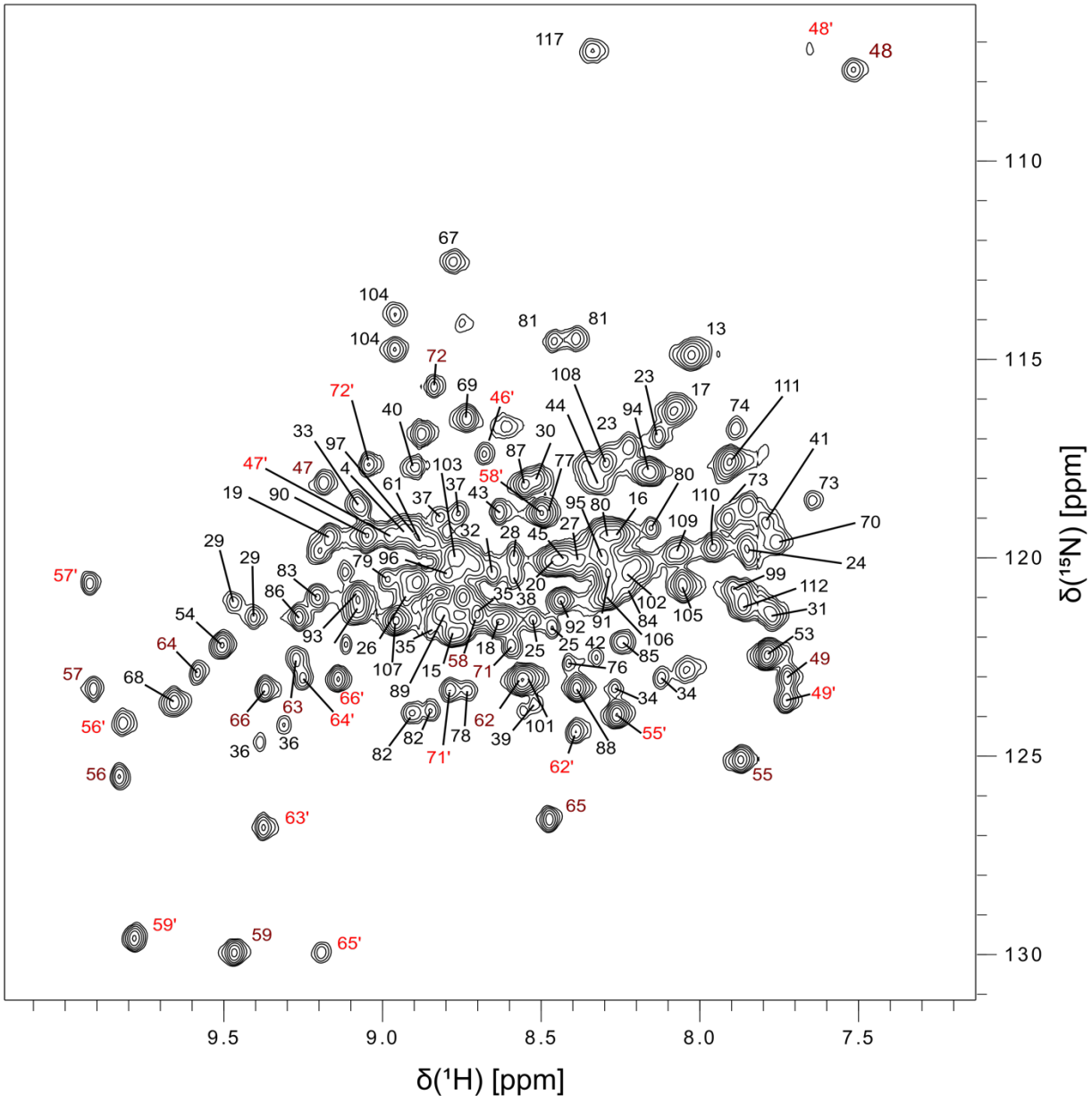

References

Amero C, Schanda P, Dura MA, et al (2009) Fast two-dimensional NMR spectroscopy of high molecular weight protein assemblies. Journal of The American Chemical Society 131:3448–3449. https://pubs.acs.org/doi/10.1021/ja809880p

Ayala I, Chiari L, Kerfah R, et al (2020) Asymmetric Synthesis of Methyl Specifically Labelled *L* -Threonine and Application to the NMR Studies of High Molecular Weight Proteins. ChemistrySelect 5:5092–5098. https://doi.org/10.1002/slct.202000827

Ayala I, Sounier R, Usé N, et al (2009) An efficient protocol for the complete incorporation of methyl-protonated alanine in perdeuterated protein. Journal of Biomolecular NMR 43:111–119. https://doi.org/10.1007/s10858-008-9294-7

Comyn SA, Young BP, Loewen CJ, Mayor T (2016) Prefoldin Promotes Proteasomal Degradation of Cytosolic Proteins with Missense Mutations by Maintaining Substrate Solubility. PLoS Genetics 12(7): e1006184 https://doi.org/10.1371/journal.pgen.1006184

Delaglio F, Grzesiek S, Vuister GeertenW, et al (1995) NMRPipe: A multidimensional spectral processing system based on UNIX pipes. Journal of Biomolecular NMR 6:277–293. https://doi.org/10.1007/BF00197809

Djohan Y, Azukizawa T, Patmawati P, et al (2019) Molecular chaperone prefoldin-assisted biosynthesis of gold nanoparticles with improved size distribution and dispersion. Biomaterials Science 7:1801–1804. https://doi.org/10.1039/C8BM01026A

Favier A, Brutscher B (2019) NMRlib: user-friendly pulse sequence tools for Bruker NMR spectrometers. Journal of Biomolecular NMR 73:199–211. https://doi.org/10.1007/s10858-019-00249-1

Gans P, Hamelin O, Sounier R, et al (2010) Stereospecific Isotopic Labeling of Methyl Groups for NMR Spectroscopic Studies of High-Molecular-Weight Proteins. Angewandte Chemie International Edition 49:1958–1962. https://doi.org/10.1002/anie.200905660

Kerfah R, Hamelin O, Boisbouvier J, Marion D (2015a) CH3-specific NMR assignment of alanine, isoleucine, leucine and valine methyl groups in high molecular weight proteins using a single sample. Journal of Biomolecular NMR 63:389–402. https://doi.org/10.1007/s10858-015-9998-4

Kerfah R, Plevin M j., Sounier R, et al (2015b) Methyl Specific Isotopic Labeling: A Molecular Tool Box for NMR Studies of Large Proteins Authors: Current Opinion in Structural Biology 32:113-22. https://doi.org/10.1016/j.sbi.2015.03.009

Korzhnev DM, Kloiber K, Kanelis V, et al (2004) Probing Slow Dynamics in High Molecular Weight Proteins by Methyl-TROSY NMR Spectroscopy: Application to a 723-Residue Enzyme. Journal of the American Chemical Society 126:3964–3973. https://doi.org/10.1021/ja039587i

Lee YS, Smith RS, Jordan W, et al (2011) Prefoldin 5 is required for normal sensory and neuronal development in a murine model. Journal of Biological Chemistry 286:726–736. https://doi.org/10.1074/jbc.M110.177352

Leroux MR (1999) MtGimC, a novel archaeal chaperone related to the eukaryotic chaperonin cofactor GimC/prefoldin. The EMBO Journal 18:6730–6743. https://doi.org/10.1093/emboj/18.23.6730

Lescop E, Schanda P, Brutscher B (2007) A set of BEST triple-resonance experiments for time-optimized protein resonance assignment. Journal of Magnetic Resonance 187:163–169. https://doi.org/10.1016/j.jmr.2007.04.002

Lundin VF, Srayko M, Hyman AA, Leroux MR (2008) Efficient chaperone-mediated tubulin biogenesis is essential for cell division and cell migration in C. elegans. Developmental Biology 313:320–334. https://doi.org/10.1016/j.ydbio.2007.10.022

Lundin VF, Stirling PC, Gomez-Reino J, et al (2004) Molecular clamp mechanism of substrate binding by hydrophobic coiled-coil residues of the archaeal chaperone prefoldin. Proceedings of the National Academy of Sciences of the United States of America 101:4367–72. https://doi.org/10.1073/pnas.0306276101

Martín-Benito J, Boskovic J, Gómez-Puertas P, et al (2002) Structure of eukaryotic prefoldin and of its complexes with unfolded actin and the cytosolic chaperonin CCT. EMBO Journal 21:6377–6386. https://doi.org/10.1093/emboj/cdf640

Martín-Benito J, Gómez-Reino J, Stirling PC, et al (2007) Divergent Substrate-Binding Mechanisms Reveal an Evolutionary Specialization of Eukaryotic Prefoldin Compared to Its Archaeal Counterpart. Structure 15:101–110. https://doi.org/10.1016/j.str.2006.11.006

Mas G, Crublet E, Hamelin O, et al (2013) Specific labeling and assignment strategies of valine methyl groups for NMR studies of high molecular weight proteins. Journal of Biomolecular NMR 57:251–262. https://doi.org/10.1007/s10858-013-9785-z

Millán-Zambrano G, Chávez S (2014) Nuclear functions of prefoldin. Open Biology 4: 140085. https://doi.org/10.1098/rsob.140085

Monneau YR, Rossi P, Bhaumik A, et al (2017) Automatic methyl assignment in large proteins by the MAGIC algorithm. Journal of Biomolecular NMR 69:215–227. https://doi.org/10.1007/s10858-017-0149-y

Ohtaki A, Kida H, Miyata Y, et al (2008) Structure and Molecular Dynamics Simulation of Archaeal Prefoldin: The Molecular Mechanism for Binding and Recognition of Nonnative Substrate Proteins. Journal of Molecular Biology 376:1130–1141. https://doi.org/10.1016/j.jmb.2007.12.010

Okochi M, Yoshida T, Maruyama T, et al (2002) Pyrococcus prefoldin stabilizes protein-folding intermediates and transfers them to chaperonins for correct folding. Biochemical and Biophysical Research Communications 291:769–774. https://doi.org/10.1006/bbrc.2002.6523

Saibil H (2013) Chaperone machines for protein folding, unfolding and disaggregation. Nature reviews Molecular cell biology 14:630–42. https://doi.org/10.1038/nrm3658

Sakono M, Zako T, Ueda H, et al (2008) Formation of highly toxic soluble amyloid beta oligomers by the molecular chaperone prefoldin. FEBS Journal 275:5982–5993. https://doi.org/10.1111/j.1742-4658.2008.06727.x

Shokuhfar A, Ghaffari A, Ghasemi RH (2012) Cavity Control of Prefoldin Nano Actuator (PNA) by Temperature and pH. Nano-Micro Letters 4:110–117. https://doi.org/10.1007/BF03353701

Siegert R, Leroux MR, Scheufler C, et al (2000) Structure of the Molecular Chaperone Prefoldin. Cell 103:621–632. https://doi.org/10.1016/S0092-8674(00)00165-3

Sörgjerd KM, Zako T, Sakono M, et al (2013) Human prefoldin inhibits amyloid-β (Aβ) fibrillation and contributes to formation of nontoxic Aβ aggregates. Biochemistry 52:3532–3542. https://doi.org/10.1021/bi301705c

Takano M, Tashiro E, Kitamura A, et al (2014) Prefoldin prevents aggregation of α-synuclein. Brain Research 1542:186–194. https://doi.org/10.1016/J.BRAINRES.2013.10.034

Tashiro E, Zako T, Muto H, et al (2013) Prefoldin protects neuronal cells from polyglutamine toxicity by preventing aggregation formation. Journal of Biological Chemistry 288:19958–19972. https://doi.org/10.1074/jbc.M113.477984

Törner R, Awad R, Gans P, et al (2020) Spectral editing of intra- and inter-chain methyl–methyl NOEs in protein complexes. Journal of Biomolecular NMR 74: 83–94. https://doi.org/10.1007/s10858-019-00293-x

Tugarinov V, Choy WY, Orekhov VY, Kay LE (2005) Solution NMR-derived global fold of a monomeric 82-kDa enzyme. Proceedings of the National Academy of Sciences of the United States of America 102:622–627. https://doi.org/10.1073/pnas.0407792102

Tugarinov V, Hwang PM, Ollerenshaw JE, Kay LE (2003) Cross-correlated relaxation enhanced 1H-13C NMR spectroscopy of methyl groups in very high molecular weight proteins and protein complexes. Journal of the American Chemical Society 125:10420–10428. https://doi.org/10.1021/ja030153x

Vainberg IE, Lewis SA, Rommelaere H, et al (1998) Prefoldin, a chaperone that delivers unfolded proteins to cytosolic chaperonin. Cell 93:863–73. https://doi.org/10.1016/S0092-8674(00)81446-4

Vranken WF, Boucher W, Stevens TJ, et al (2005) The CCPN data model for NMR spectroscopy: Development of a software pipeline. Proteins: Structure, Function, and Bioinformatics 59:687–696. https://doi.org/10.1002/prot.20449

Yébenes H, Mesa P, Muñoz IG, et al (2011) Chaperonins: two rings for folding. Trends in biochemical sciences 36:424–32. https://doi.org/10.1016/j.tibs.2011.05.003

Zako T, Iizuka R, Okochi M, et al (2005) Facilitated release of substrate protein from prefoldin by chaperonin. FEBS Letters 579:3718–3724. https://doi.org/10.1016/j.febslet.2005.05.061

Zako T, Murase Y, Iizuka R, et al (2006) Localization of Prefoldin Interaction Sites in the Hyperthermophilic Group II Chaperonin and Correlations between Binding Rate and Protein Transfer Rate. Journal of Molecular Biology 364:110–120. https://doi.org/10.1016/j.jmb.2006.08.088

Zako T, Sahlan M, Fujii S, et al (2016) Contribution of the C-Terminal Region of a Group II Chaperonin to its Interaction with Prefoldin and Substrate Transfer. Journal of Molecular Biology 428:2405–2417. https://doi.org/10.1016/j.jmb.2016.04.006